3-D Numerical Simulation of Main Sieve Diaphragm with three types Passageway Design in a Gas Mask Canister

Chun-Chi Li[1], Jr-Ming Miao[1], Chin-Chiang Wang[2], Yin-Chia Su[2], and Tzu-Yi Lo[2]

[1] Department of Mechatronic , Energy and Aerospace Engineering , Chung Cheng Institute of Technology, National Defense University, Taiwan, R.O.C (email:davidli@ndu.edu.tw)
[2] Master Program of Mechanical Engineering, Chung Cheng Institute of Technology, National Defense University, Taiwan, R.O.C

Abstract. This paper focuses on the passageway design of the main sieve diaphragm that is the key point to reduce the pressure drop of a gas mask canister. Three types of the passageways are designed to explore the aerodynamic behaviors of the flow inside a canister. The models include the hole, rib-strip and honeycomb types. The 3-D numerical simulations of flows have been applied to determine the pressure drops in the models. The simulation results reveal the smallest pressure drops on the passageway of honeycomb type, because the structure of honeycomb type is stronger enough to avoid the deformation of the main sieve diaphragm. So the passageway of honeycomb type can provide larger channel area and more uniform channel distribution to reduce the pressure drop. The analysis of the flow structure, such as the velocity profile and the distribution of dead zone in the models, is also studied.
Keywords: main sieve diaphragm, gas mask canister, porous media, air age

1 Introduction

After the 911 terror-attack, the gas masks are not only for soldiers to use in the battle fields, but also for people to regard these masks as necessities for their daily lives. Therefore, the gas masks are bringing the potential commercial opportunities in the markets. On the basis of the design of gas mask and in addition to confirming the standard of toxic filtering, the low pressure drop of respiratory is the other considerable factor. The pressure drop of a gas mask mainly results from inhaling gas through the canister. The canister generally consists of the filter layer and activated carbon layer. Both layers are defined as porous media significantly causing the pressure drop. The filter layer consists of multi-pleated filter papers enabling to block suspended particles. The activated carbon layer can functionally adsorb and filter toxic gases. Generally, to connect the filter layer and the activated carbon layer is a main sieve diaphragm that is an only passageway to permit gas entering activated carbon layer.
To the design of this kind of porous media filters, like gas mask canister or industrial filters, the aerodynamic behaviors of fluids, such as pressure drop and flow structure, are the most vital factors in the flow dynamic system [1]. The flow

structures should prevent from forming the preferential flow and the dead zone. Due to the opaqueness of the absorbent, it would not be experimentally observed the inner flow structures through the sizes and locations of the preferential flow and dead zones. It will be helpful to explore the aerodynamic characteristics of the flow field for the references of the design and improvement, through employing the CFD tools to analyze the flow variables in porous media inside the filter. According to the fluid dynamics of porous media, it generally obeys the Darcy's equation at low Reynolds number. In this equation, the pressure drop is satisfied with the linear relation as below.

$$-\Delta P/L = (\mu/\kappa)V_s \tag{1}$$

where ΔP is the pressure drop of porous medium zone, L is the length in flow direction, κ is the permeability, μ is the fluid viscosity and V_s is the superficial velocity entering porous medium zone.
When the superficial velocity or Reynolds number increases, the inertia effect is gradually to increase. A second order parabolic equation can describe the inertia effect that is called the Forchheimer's equation, shown as below.

$$-\Delta P/L = \alpha\mu V_s + \beta\rho V_s^2 \tag{2}$$

where α is the reciprocal permeability of porous material, it also called viscous parameter. β is usually called the inertial parameter.
Previous authors have used CFD tools to analyze porous filters, but their primary focus was to analyze the fluids flow through different arrays of the spatial microstructure of a filter media in 2-D or 3-D simulations [2-4].The point which most previous studies have in common is that they focused on a single type of porous media. However, very little existing literature analyzes the aerodynamic characteristics of a gas mask canister. Therefore, the topic of the aerodynamic behavior of a gas mask canister with two kinds porous materials is worthy of further research.
Li & Liao, used CFD to simulate a gas mask canister containing two porous media [5]. The passageway of main sieve diaphragm in the canister was hole type. The effects of the distribution and area of holes in the main sieve diaphragm and the thickness of the activated carbon layer on the pressure drop and the aerodynamic flow behavior inside the canister body were determined. The results revealed the flow structures in the activated carbon layer were dominated by the passageway distribution of main sieve diaphragm. Better hole distribution and a larger hole area corresponded to a lower pressure drop, a smaller dead zone, and a higher adsorption time. In present study, we design three types of the passageways to explore the aerodynamic behaviors of the flow inside a canister. The design of passageway on main sieve diaphragm should be optimized by considering not only how to reduce the pressure drop and the weight of activated carbon layer, but also the structural strength and the limitations of the manufacturing technique used. The analysis of the flow structure, such as the velocity profile and the distribution of dead zone in the models, is also studied.

2 Problem

2.1 Governing equations

The governing equations herein include the continuity and momentum equations, both of which obey the conservation principle,

$$\frac{\partial}{\partial x_i}(\rho u_i) = 0 \ , \tag{3}$$

$$\frac{\partial}{\partial x_j}(\rho u_i u_j) = -\frac{\partial P}{\partial x_i} + \frac{\partial \tau_{ij}}{\partial x_j} + \rho g_i - \frac{\partial}{\partial x_j}(\rho \overline{u_i' u_j'}) + S_i \ , \tag{4}$$

where ρ is the fluid density; u_i is the velocity component in the i direction;p is the pressure; τ_{ij} is the viscosity shear stress tensor; g_i is the acceleration due to gravity in the i direction; $\rho\overline{u_i' u_j'}$ is the Reynolds stress term, related to the mean flow by the Boussinesq hypothesis when the flow is not laminar, and S_i is a source term that describes the pressure gradient in the porous medium, and is defined by Eq. (2) and is assumed to be isotropic. The turbulent model is adopted the $\kappa - \varepsilon$ turbulent model with low-Reynolds number[6]. The working gas is air, for which $\rho = 1.225 kg\, m^{-3}$ and $\mu = 1.7894 \times 10^{-5} kg\, m^{-1} s^{-1}$.
The air age equation is

$$\frac{\partial}{\partial x_i}(\rho u_i \tau) = \frac{\partial}{\partial x_i}(\frac{\mu_{eff}}{\sigma_\tau}\frac{\partial_\tau}{\partial x_i}) + \rho \ , \tag{5}$$

where τ is the air age; $\mu_{eff} = \mu_l + \mu_t$ (where μ_{eff} is effective viscosity, μ_l is molecular viscosity and μ_t is turbulent viscosity) and $\sigma_\tau = 1$ is the turbulent Schmidt number.

2.2 Boundary conditions & Numerical method

At the inlet of the canister, a constant velocity value is imposed. The outlet boundary condition is the outlet pressure boundary. The no-slip condition was assumed at the solid wall. The central axial plane of the canister is regarded as a symmetrical boundary.
The 3-D numerical simulations of flows have been applied to determine the pressure drops in the models. The flow variables in present models are solved by the Navier-Stokes equations adding to the low Reynolds number $\kappa - \varepsilon$ turbulent model. The pressure gradient is calculated by Forchheimer's equation to add to the source term of the momentum equation. The air age is employed to represent the resident time of gas in a canister. The finite volume method based on the cell center is used in the models. We discretize the integral form governing equations based on unstructured tetrahedron grid. The convection term is discretized by the one-order upwind scheme and the viscous term is discretized by central differential scheme. The solution algorithm for pressure-velocity coupling is the SIMPLE algorithm and related discretization algebraic equations are solved using the TDMA method.

2.3 Grid configuration

According to the research of Li & Liao, we know the passageway design of the main sieve diaphragm that is the key point to reduce the pressure drop of a canister. In this paper, three types of passageways are designed to explore the aerodynamic behaviors of the flow inside a canister. The mesh of models including the hole, rib-strip and honeycomb types are shown in Figure 1. All the results presented here are grid-independent. The residual convergence criterion in all cases was less than 1×10^{-4}.

3 Result & Discussion

We used curve fitting to estimate the viscous and inertia parameters of the porous media in accordance with the experimental data. The simulation results of the estimated inertial and viscosity parameters in the Forchheimer's equation are in good agreement with the experiment. The more details see the [5]. In the following simulations, the same parameters are used. Figure 2(a-c) shows the velocity contours of hole, honeycomb and rib-strip types at the flow rate of 30 L/min. Figure 2(a) shows that since the outermost holes are sealed and and the porous flow causes momentum loss, the gas flowing through the open holes of the main sieve diaphragm does not easily flow past the outer part of the activated carbon layer. Thus, a larger low-velocity zone called dead zone forms in this area. Figure 2(b) shows that the rib-strip design of the main sieve diaphragm in models H_1, the original low-velocity region in Fig 2(a) decreases in size. Figure 2(c) shows that the honeycomb design of the main sieve diaphragm in models J_1, the low-velocity region almost disappears.
Employing the flow variable distributions described by the air age index, it is much easier to judge the position of the dead zone through observing the flow structure inside the activated carbon layer. Figure 3(a-c) appears the contours of air ages of the hole, rib-strip and honeycomb types. Models A_1, with sealed outermost holes, clearly have a large zone of higher air age outside the activated carbon layer (Fig. 3(a)). The gas cannot flow easily through this zone, and a large dead zone is formed. Figure 3(b) shows that the original dead zone in Fig 3(a) apparently shrinks, but a little dead zone still exists at the corner of wall. Figure 3(c) shows that the dead zone almost disappears in Model J_1. Figure 4 shows the velocity profile of three type passageways. The velocity profile of honeycomb type is more uniform than those of others. The local parts of high or low velocity profiles form the preferential flow or the dead zones result in increasing the pressure drops of a canister.

4 Conclusion

Equations for a porous medium describe the relationship between the superficial velocity and the pressure drop from a macro perspective. A higher superficial

velocity corresponds to a greater pressure drop. According to the continuity equation, the product of the superficial velocity and the flow-through area yields the volumetric flow rate. Consider model A_1 as an example: the passageway of main sieve diaphragm yields a non-uniform velocity profile. Fluid does not flow easily into the resulting low-velocity zone, yielding a dead zone. Hence, the overall superficial velocity in the activated carbon layer increases, increasing the pressure drop. In contrast, the passageway of honeycomb design yields a more uniform velocity profile, as in model J_1, reducing the size of the dead zone, and reducing the superficial velocity in the activated carbon layer, thereby reducing the pressure drop. Using the advantages of CFD, the positions of the dead zones and the preferential flow can be identified, providing great assistance in the design of improved main sieve diaphragms.

To summarize the research results, the conclusions can be obtained as follows: comparing with the three types of the passageways, because the structure of honeycomb type is stronger enough to avoid the deformation of main sieve diaphragm, so the main sieve diaphragm of the honeycomb type own the larger channel area and better channel distribution to reduce the pressure drop.

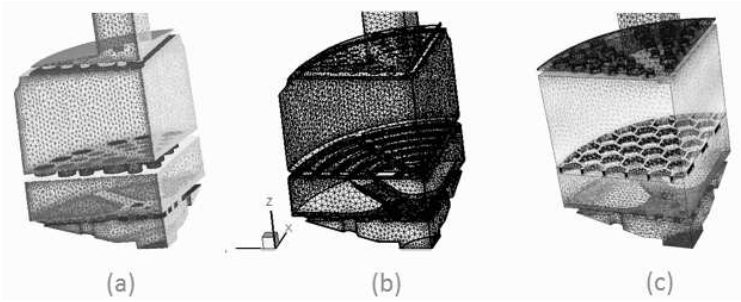

Fig. 1. Mesh system of three types of passageways on a gas mask canister. ((a) hole type, (b) rib-strip-type and (c) honeycomb type)

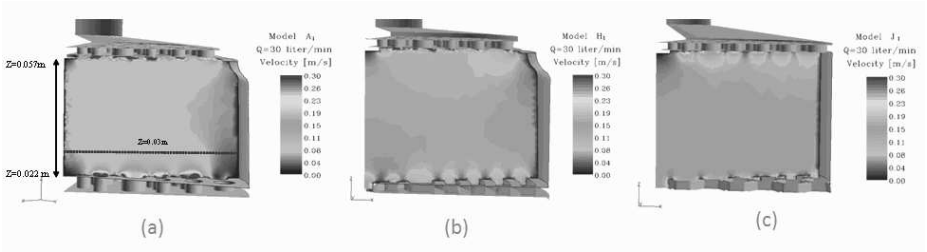

Fig. 2. The velocity contours in the activated carbon layer under the condition of flow rate, 30 L/min. ((a) hole type, (b) rib-strip-type and (c) honeycomb type)

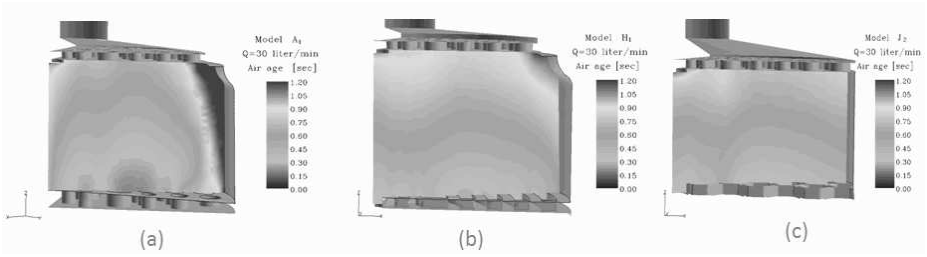

Fig. 3. The air age contours in the activated carbon layer under the condition of flow rate, 30 L/min. ((a) hole type, (b) rib-strip-type and (c) honeycomb type)

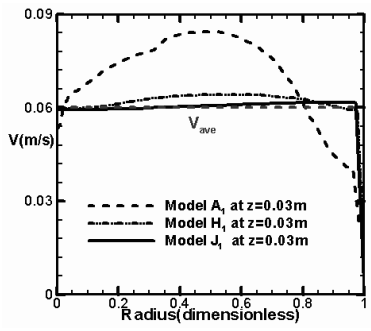

Fig. 4. Velocity profile of three types of models at 30 L/min.

References

1. A. Subrenat, J. Bellettre, P. Le Cloirec : 3-D numerical simulations of flow in a cylindrical pleated filter packed with activated carbon cloth. *Chemical Engineering Science,58,* pp. 4965–4973.(2003)
2. S. Dhaniyala, B.Y.H. Liu : An asymmetrical, three-dimensional model for fibrous filters. *Aerosol Science and Technology, 30(4),* pp. 333–348.(1999)
3. Z.G. Liu, P.K. Wang : Numerical investigation of viscous flow fields around multi-fiber filters. *Aerosol Science and Technology, 25(4)*, pp. 375–391.(1996)
4. D. Thomas, P. Contal, V. Renaudin, P. Penicot, D. Leclerc, J. Vendel : Modelling pressure drop in HEPA filters during dynamic filtration. *Journal Aerosol Science, 30(2)*, pp. 235–246.(1999)
5. C.C. Li, K.C. Lio : Aerodynamic behavior of a gas mask canister containing two porous media. *Chemical Engineering Sci.,* (submitted).(2008)
6. W.P. Jones, B.E. Launder : The calculation of low-Reynolds-number phenomena with a two-equation model of turbulence. *Int. Journal Heat Mass Transfer, 16,* pp. 1119–1130.(1973)